Friction phenomena in a two-dimensional Frenkel–Kontorova model*

Lin Mai-Mai(林麦麦)[a)†], Duan Wen-Shan(段文山)[a)], and Chen Jian-Min(陈建敏)[b)]

[a)] *Department of Physics, Northwest Normal University, Lanzhou* 730070, *China*
[b)] *State Key Laboratory of Solid Lubrication, Lanzhou Institute of Chemical Physics, Chinese Academy of Sciences, Lanzhou* 730000, *China*

(Received 12 June 2009; revised manuscript received 10 July 2009)

By using the molecular dynamic simulation method with a fourth-order Runge–Kutta algorithm, a two-dimensional dc- and ac-driven Frenkel–Kontorova (FK) model with a square symmetry substrate potential for a square lattice layer has been investigated in this paper. For this system, the effects of many different parameters on the average velocity and the static friction force have been studied. It is found that not only the amplitude and frequency of ac-driven force, but also the direction of the external driving force and the misfit angle between two layers have some strong influences on the static friction force. It can be concluded that the superlubricity phenomenon appears easily with a larger ac amplitude and lower ac frequency for some special direction of the external force and misfit angle.

Keywords: Frenkel–Kontorova model, static friction force, Runge–Kutta method

PACC: 6220P, 8140P, 4630P

1. Introduction

Nowadays, the investigations of friction phenomenon perhaps become one of the greatest challenges to the scientific and industrial communities among all physical problems.[1−12] As is well known, the Frenkel–Kontorova (FK) model is one of the simplest but still complex enough models to capture the essence of many physical phenomena including friction phenomenon. The dynamical behaviours of many-body systems in the FK model have been extensively studied both theoretically and experimentally.[1] The standard one-dimensional FK model represents a chain of harmonically interacting particles subjected to an external periodic (sinusoidal) substrate potential.[13] Many theoretical and experimental investigations have shown that there are very rich dynamical behaviours in the FK model under an external driving force with different commensurate or incommensurate structures.[14−17] Contrary to a large number of studies for the dc-driven FK model, a relatively small number of researches have been focused on the FK model with dc- and ac-driven force. Floría *et al.* have studied the one-dimensional standard FK model submitted to dc and ac forces with both commensurate and incommensurate structures.[18−20] This is possibly because the ac–dc interference phenomena and the Shapiro steps have become one of the extensive theoretical and experimental studies in the dissipative dynamics of the many-body system with competing interactions.[18−20] The ac–dc FK model can also be used in tribology. The ac-driven force can be considered as external vibration or some regular disturbances, and we want to know how these vibrations or disturbances affect the static friction force.

The amplitude and frequency dependence of dynamical mode locking phenomena in the dc- and ac-driven overdamped FK model is investigated by Hu *et al.*[21] Tekić *et al.* also studied the frequency dependence of the dynamical-mode-locking phenomena in the presence of noise for the one-dimensional dissipative FK model.[22]

However, in friction systems, the importance of higher dimensionality has been emphasized, which makes the superlubricity (the state of vanishing friction) appear much more easily.[23,24] It is found in the experimental results that by measuring the atomic-scale friction force as a function of rotational angle between two contacting surface layers superlubricity may appear in a certain misfit angle.[23,24] Higher dimensionality of the system is, therefore, crucial in the study of friction phenomena. It is necessary to extend the one-dimensional FK model to the higher dimen-

*Project supported by the National Natural Science Foundation of China (Grand Nos. 50575217, 10875098 and 50421502), and the Natural Science Foundation of Northwest Normal University (Grant Nos. NWNU-KJCXGC-03-17 and NWNU-KJCXGC-03-48).
†Corresponding author. E-mail: linmaimai@nwnu.edu.cn
© 2010 Chinese Physical Society and IOP Publishing Ltd

sions to obtain a more real case which can be realized. Moreover, the study of dynamical behaviour in the two-dimensional (2D) FK model has drawn much attention since it may be a possible interpretation for understanding the more complex problems of the nanotribology field.[25,26] Because of these reasons, in this paper, a two-dimensional dc- and ac-driven FK model with a square symmetry substrate potential for a square lattice layer has been studied. We are particularly interested in how the amplitude and frequency of the ac-driven force, as well as the misfit angle and the direction of the external driving force affect the static friction force. It is found that for certain ac amplitudes and frequencies the static friction force can be very small. It indicates that superlubricity is possible for us to choose appropriate ac-driven force.

This paper is organized as follows: in Section 2, a two-dimensional FK model with dc- and ac-driven forces has been introduced. In Section 3, the simulation results are presented. The effects of different parameters (such as the ac amplitude, the ac frequency, the direction of external driving force, and the misfit angle, and so on) on the average velocity and the static friction force have been investigated in detail for different cases. In Section 4, the main conclusions have been concluded briefly.

2. Model

In order to study the effect of ac-driven force on the static friction force, we consider the atoms which are arranged on a two-dimensional square lattice (the upper layer) as discussed in Ref. [4]. The atoms in the upper layer not only interact each other, but also interact with a periodic substrate potential (the lower layer). For simplicity, we assume that the position of an arbitrary (n,m)-th atom is $\boldsymbol{r}_{n,m} = (x_{n,m}, y_{n,m})$ which satisfies the following equation of motion[4]

$$m\ddot{\boldsymbol{r}}_{n,m} + \gamma\dot{\boldsymbol{r}}_{n,m} + \frac{\partial(V_{\rm int} + V_{\rm sub})}{\partial \boldsymbol{r}_{n,m}} = \boldsymbol{F}_{\rm ext}, \qquad (1)$$

where m is the mass of atom and γ is a phenomenology viscous damping coefficient. $V_{\rm int}$ refers to the interatomic interaction among the upper layer. It is assumed to be a simple harmonic form:

$$V_{\rm int} = \sum_{i,j} \frac{K}{2}\left[(x_{i,j} - x_{n,m} - a)^2 + (y_{i,j} - y_{n,m} - a)^2\right],$$

where K is a stiffness strength between two atoms in the upper layer, a is a natural equilibrium spacing of the upper layer. $V_{\rm sub}$ is the substrate potential of the lower layer. We assume that $V_{\rm sub}$ is in the simple sinusoidal form with the square lattice symmetry as follows:

$$V_{\rm sub} = \frac{f}{2\pi}\left(\cos\frac{2\pi x'}{b} + \cos\frac{2\pi y'}{b}\right),$$

where f is the magnitude of the lateral corrugation of the substrate potential, b defines a natural equilibrium spacing of the lower layer. In order to study the general case of this system, we rotate the two layers with respect to each other by an arbitrary misfit angle θ. Then the substrate potential becomes:

$$V_{\rm sub} = \frac{f}{2\pi}\left[\cos\frac{2\pi(x\cos\theta - y\sin\theta)}{b} + \cos\frac{2\pi(x\sin\theta + y\cos\theta)}{b}\right].$$

The external driving force $\boldsymbol{F}_{\rm ext} = (F_{\rm ext}\cos\alpha, F_{\rm ext}\sin\alpha)$ with α being the angle between the force $\boldsymbol{F}_{\rm ext}$ and the unit vector of x-axis. In order to investigate the dc- and ac-driven FK model, we assume that the external driving force can be written as:

$$F_{\rm ext} = F_{\rm dc} + F_{\rm ac}\cos(2\pi\nu_0 t),$$

where $F_{\rm dc}$ is the dc-driven force, $F_{\rm ac}$ and ν_0 refer to the amplitude and frequency of ac-driven force, respectively.

3. Results

Now, we solve Eq. (1) numerically by using a fourth-order Runge–Kutta algorithm. The atoms were initially at its equilibrium positions, then the external driving force $\boldsymbol{F}_{\rm ext}$ was increased adiabatically with steps $\mathrm{d}F_{\rm ext} = 0.005$, allowing a sufficiently long time $t = 300$ (time step $\mathrm{d}t = 0.006$) to equilibrate at each new value of $F_{\rm ext}$, where the values of parameters are: $\gamma = 0.1$, $K = 5$, $f = 1$, $a = 1$ and $b = 1$ respectively. The average velocity $\bar{\boldsymbol{v}}$ is defined as

$$\bar{\boldsymbol{v}} = \frac{1}{N \times M}\sum_{i=1,j=1}^{i=N,j=M}\langle\dot{\boldsymbol{x}}_{i,j}\rangle,$$

where $\langle\ \rangle$ denotes the time average. The interparticle equilibrium length a, not explicitly entering Eq. (1), appears only via the boundary conditions: $x_{M+1} = x_1 + Ma$ and $y_{M+1} = x_1 + Na$ (where M, N are integers), to enforce a fixed density condition for this system. We model the atomic layer by letting $N = 10$,

$M = 10$ and analyse the locked-to-sliding transition for different values of the system parameters. Following the previous studies in one-dimensional FK model, we explore the commensurate case ($\beta \equiv b/a = 1$).

The effects of the amplitude and frequency of the ac driven force on the average velocity for different cases are shown in Figs. 1 and 2 respectively. In Fig. 1, the amplitude of the mean velocity $\bar{v}$ for the commensurate structure are presented for different amplitude of ac-driven forces. It is shown that, for a given values of α (where $\alpha = 45°, 30°, 15°$ respectively), the static friction force $F_{\rm s}$ decreases as the amplitude of ac force $F_{\rm ac}$ increases. Meanwhile, as shown in Fig. 1, the static friction force $F_{\rm s}$ increases as α increases from 0° to 45°. It indicates that both the ac amplitude and the direction of external driving force strongly influence the average atom velocity and the magnitude of static friction force.

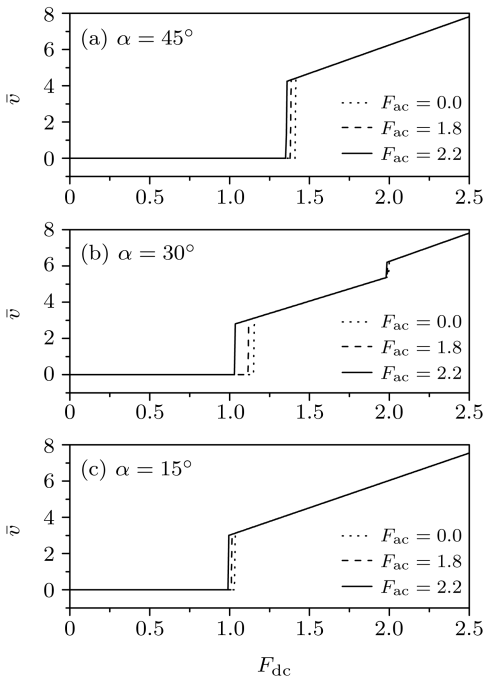


Fig. 1. The average velocity $\bar{v}$ as a function of $F_{\rm dc}$ with different ac amplitude $F_{\rm ac} = 0.0, 1.8, 2.2$, where $\theta = 0°, \nu_0 = 1.0$ for three cases: (a) $\alpha = 45°$, (b) $\alpha = 30°$, and (c) $\alpha = 15°$, respectively.

Figure 2 shows the average velocity $\bar{v}$ with respect to $F_{\rm dc}$ for different values of frequency of ac driven force. It is shown that as the frequency ν_0 increases the static friction force $F_{\rm s}$ increases for the case of $\alpha = 45°$ and 30°. On the other hand, as shown in Fig. 2(c), where $\alpha = 15°$, $F_{\rm s}$ decreases as the ac frequency ν_0 increases from 0.2 to 0.4, but increases as the ac frequency increases from 0.4 to 0.8. As a conclusion from Figs. 1 and 2, both the amplitude and the frequency of ac-driven force have obvious effect on the static friction force and the mean velocity of the upper layer. Moreover, the direction of external driving force also has important effect on both the static friction force and the mean velocity of the upper layer.

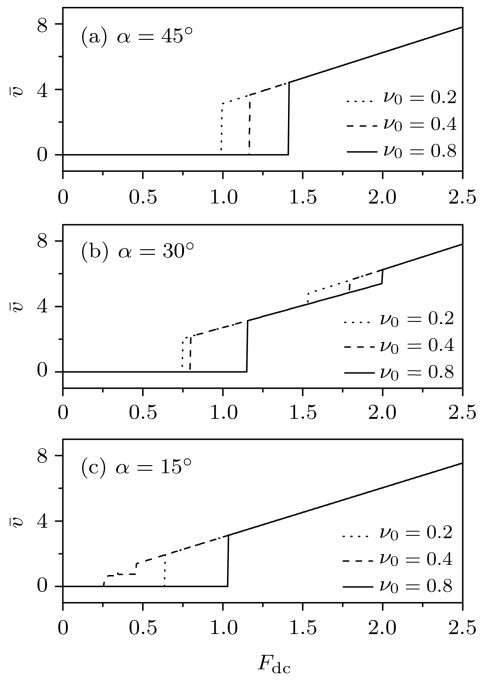


Fig. 2. The average velocity $\bar{v}$ as a function of $F_{\rm dc}$ with different ac frequencies $\nu_0 = 0.2, 0.4, 0.8$ where $\theta = 0°, F_{\rm ac} = 0.4$ for three cases: (a) $\alpha = 45°$, (b) $\alpha = 30°$, and (c) $\alpha = 15°$, respectively.

In order to study the effect of the substrate potential on the static friction force and the average velocity of the atoms in upper layer in more detail, the dependence of the average velocity $\bar{v}$ on the $F_{\rm dc}$ for different values of both amplitude and frequency of ac driven force with different misfit angle θ are given in Figs. 3 and 4 respectively. It is noted that the misfit angle θ can significantly influence the static friction force and the average velocity of the atoms in the upper layer. Namely, the misfit angle is an important parameter which can influence the dynamical behaviours and the static friction force of this system in 2D dc- and ac-driven FK model. The reason that the average velocity of the centre of the upper layer and the static friction force strongly dependent on the misfit angle θ may be as follows: For $\theta = 0$ it is a commensurate case ($\beta = 1$), however, if $\theta \neq 0$ the commensurability is not satisfied. In most cases of $\theta \neq 0$ it is in incommensurate cases. The incommensurability is dependent on the misfit angle θ.

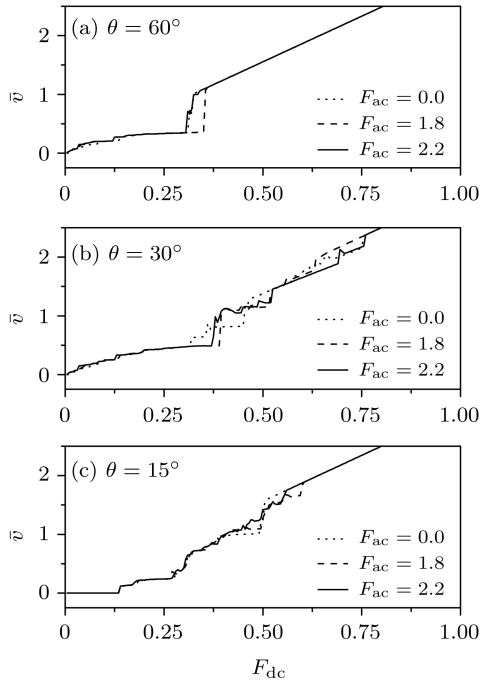


Fig. 3. The average velocity $\bar{v}$ as a function of F_{dc} with different ac amplitudes $F_{ac} = 0.0, 1.8, 2.2$, where $\alpha = 30°, \nu_0 = 1.0$ for three cases: (a) $\theta = 60°$, (b) $\theta = 30°$, and (c) $\theta = 15°$, respectively.

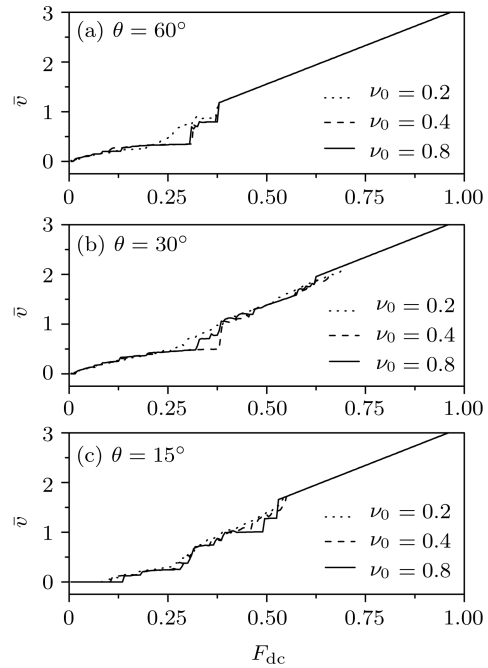


Fig. 4. The average velocity $\bar{v}$ as a function of F_{dc} with different ac frequencies $\nu_0 = 0.2, 0.4, 0.8$ with $\alpha = 30°$, $F_{ac} = 0.4$ for three cases: (a) $\theta = 60°$, (b) $\theta = 30°$, and (c) $\theta = 15°$, respectively.

The above simulation results indicate that the static friction force strongly dependent on several parameters of this system, such as the amplitude and the frequency of the ac driven force, the direction of external driving force, and the misfit angle, etc. In order to further understand it, we plot the variations of static friction force F_s with respect to amplitude F_{ac} and frequency ν_0 of the ac driven force for different cases in Figs. 5–8 respectively. Figure 5(a) shows the variations of F_s with respect to F_{ac} for different values of frequency $\nu_0 = 0.5, 0.8$, and 1.0 respectively, where $\theta = 0°, \alpha = 30°$. It is shown that the static friction force decreases as the amplitude of the ac driven force increases, however, the static friction force increases as the frequency of the ac driven force increases. In addition, the static friction force F_s tends to zero for $\nu_0 = 0.5$ as F_{ac} increases. At the same time, it is found that the static friction force $F_s < 1.2$. Figure 5(b) plots the variations of F_s with respect to F_{ac} with different system parameters of $\theta = 0°, \alpha = 15°$. The similar results are obtained as that in Fig. 5(a). However, only the maximum static friction force is different. The difference is due to the different direction of the external driving force.

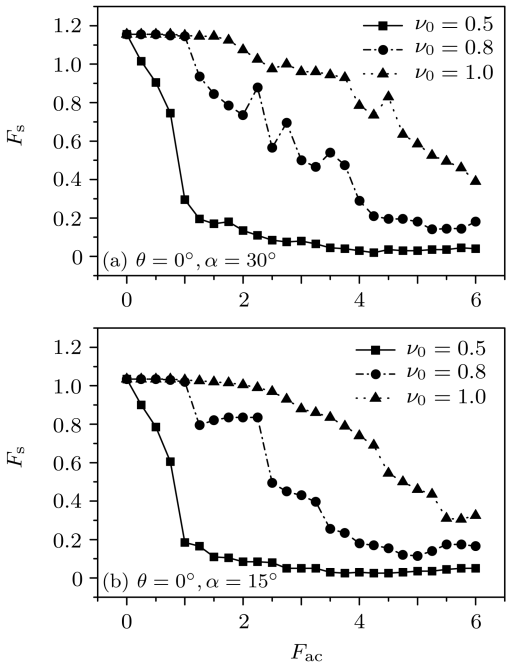


Fig. 5. The static friction force F_s as a function of the ac amplitude for different values of the ac frequency $\nu_0 = 0.5, 0.8, 1.0$ respectively: (a) $\theta = 0°$, $\alpha = 30°$, and (b) $\theta = 0°$, $\alpha = 15°$.

The variations of static friction force F_s with respect to F_{ac} for different frequencies of ac driven force and different misfit angles are plotted in Fig. 6. Figure 6(a) is the numerical results for the case of $\nu_0 = 0.5, 0.8, 1.0$ with $\theta = 30°$, $\alpha = 0°$. Compared with the case of $\theta = 0°$ in Fig. 5, we find that the maximum value of the static friction force is much smaller ($F_s < 0.07$), in which case lower static friction

force may take place. This result is similar as that reported in Ref. [4], where the ac driven force is not considered.

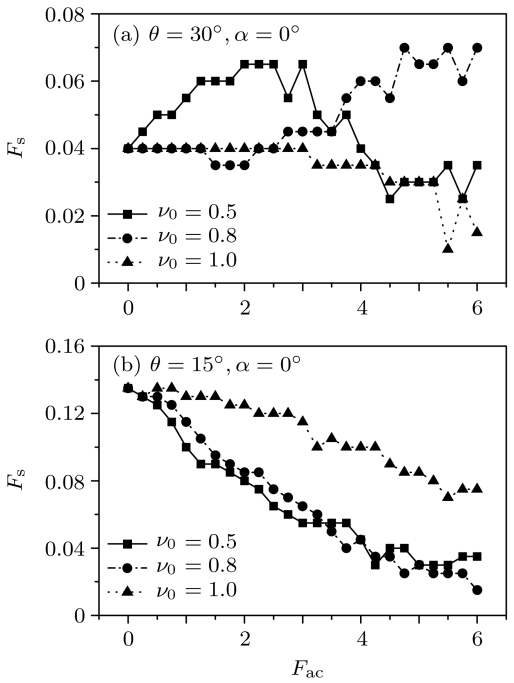


Fig. 6. The static friction force F_s as a function of the ac amplitude for different values of the ac frequency $\nu_0 = 0.5, 0.8, 1.0$ respectively: (a) $\theta = 30°$, $\alpha = 0°$, and (b) $\theta = 15°$, $\alpha = 0°$.

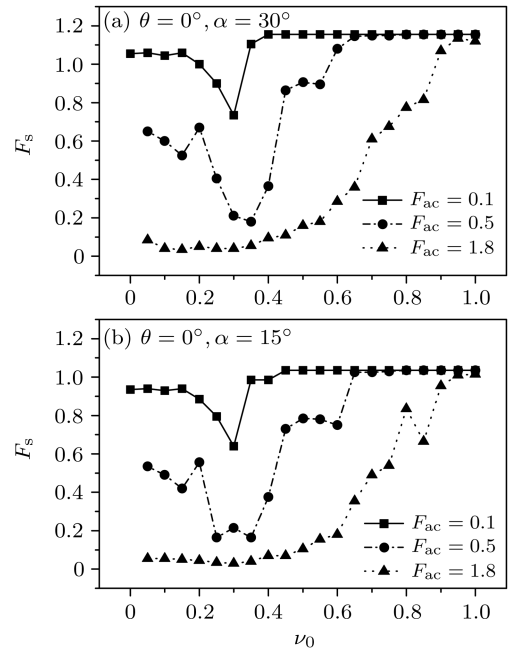


Fig. 7. The static friction force F_s as a function of the ac frequency for different values of the ac amplitude $F_{ac} = 0.1, 0.5, 1.8$ respectively: (a) $\theta = 0°, \alpha = 30°$, and (b) $\theta = 0°, \alpha = 15°$.

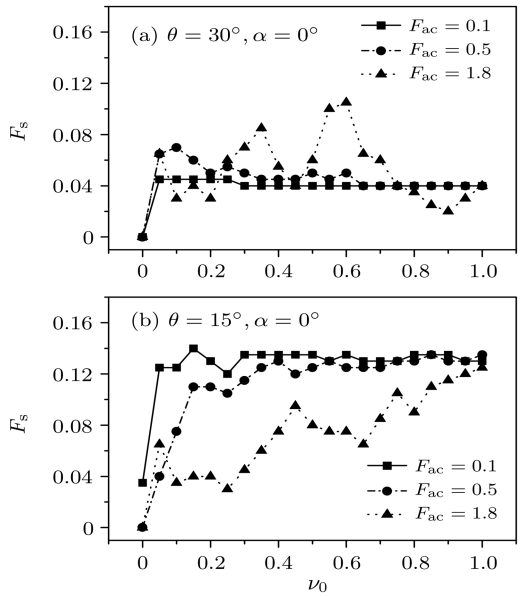


Fig. 8. The static friction force F_s as a function of the ac frequency for different values of the ac amplitude $F_{ac} = 0.1, 0.5, 1.8$ respectively: (a) $\theta = 30°, \alpha = 0°$, and (b) $\theta = 15°, \alpha = 0°$.

Meanwhile, in the case of $\nu_0 = 0.5$, F_s increases from 0.04 to 0.065 as F_{ac} increases from 0 to 2.5, then it decreases and attends to 0.025 when F_{ac} attends to 4.5. The dependence of F_s on F_{ac} in the case of $\nu_0 = 0.8$ is different from the case of $\nu_0 = 0.5$, as shown in Fig. 6(a). It is shown that the static friction force F_s is a constant value of 0.04 when $0 \leq F_{ac} \leq 1.25$, then it decreases when F_{ac} reaches to the value of 1.5, but it increases again if $F_{ac} > 2.25$ and reaches to the maximum value of 0.07 when $F_{ac} = 4.75$. For the case of $\nu_0 = 1.0$, the static friction force F_s is approximately a constant of 0.04 if $0 \leq F_{ac} \leq 3$. However, it decreases to the minimum 0.01 if the amplitude of the ac driven force further increases. Furthermore, we note that F_s approximately decreases as the frequency of the ac driven force increases when $0 \leq F_{ac} \leq 3.5$. Compared with Fig. 6(a), figure 6(b) also shows the variations of F_s with respect to F_{ac} but with different misfit angle $\theta = 15°$. It is found from Fig. 6(b) that when $0 \leq F_{ac} \leq 3.25$, F_s decreases as F_{ac} increases, but increases as ν_0 increases. This is different from that of Fig. 6(a). Therefore, we conclude that the misfit angle can strongly affect the static friction force. The variations of F_s with respect to the frequency ν_0 of the ac driven force for different amplitude of the ac driven force, the different misfit angles and the different directions of the external driving forces are shown in Figs. 7 and 8, respectively. As shown in Fig. 7 for the case of $\theta = 0°$ the static friction force decreases as the amplitude of the ac driven force increases, but

increases as the frequency of the ac driven force increases. However, it is more complex for the case of $\theta \neq 0°$, as shown in Fig. 8.

4. Conclusion

In this paper, we have studied the variations of the static friction force with different physical parameters in a two-dimensional dc- and ac-driven FK model. By using the fourth-order Runge–Kutta method, the effects of the ac-driven force, the direction of external driving force and the misfit angle on the static friction force have been discussed in detail. The numerical simulation results indicate that the lower static friction force appears easily with a larger ac amplitude and smaller ac frequency for some special direction of the external driving force and the misfit angle.

References

[1] Braun O and Kivshar Y S 1998 *Phys. Rep.* **306** 1
[2] Hu B and Tekić J 2007 *Appl. Phys. Lett.* **90** 102119
[3] Hu B, Yang L and Zhang Y 2006 *Phys. Rev. Lett.* **97** 124302
[4] Wang C L, Duan W S, Hong X R and Chen J M 2008 *Appl. Phys. Lett.* **95** 153116
[5] Hu B and Tekić J 2005 *Phys. Rev.* E **72** 056602
[6] Tekić J, Braun O M and Hu B 2005 *Phys. Rev.* E **71** 026104
[7] Hu B and Yang L 2005 *Chaos* **15** 015119
[8] Li H B, Zhao H and Wang Y H 2005 *Phys. Lett.* A **298** 361
[9] Zheng Z G, Hu B and Hu G 1998 *Phys. Rev.* B **58** 9
[10] Huang P and Xu Z M 2006 *Acta Phys. Sin.* **55** 2427 (in Chinese)
[11] Ding L Y, Gong Z L and Huang P 2008 *Acta Phys. Sin.* **57** 6500 (in Chinese)
[12] Wen S Z, Xiong Y, Zhen X J and Zhang X H 2009 *Acta Phys. Sin.* **58** 1826 (in Chinese)
[13] Braun O and Kivshar Yu S 2003 *The Frenkel–Kontorova Model* (Berlin: Springer)
[14] Braun O M, Bishop A R and Roder J 1997 *Phys. Rev. Lett.* **79** 3692
[15] Braun O M, Zhang H, Hu B and Tekíc J 2003 *Phys. Rev.* E **67** 066602
[16] Hirano M 2003 *Wear* **254** 932
[17] Li H, Xu T, Wang C, Chen J, Zhou H and Liu H 2007 *Tribology International* **40** 132
[18] Floría L M and Mazo J J 1996 *Adv. Phys.* **45** 505
[19] Falo F, Floría L M, Martínez P J and Mazo J J 1993 *Phys. Rev.* B **48** 7434
[20] Floría L M and Falo F 1992 *Phys. Rev. Lett.* **68** 2713
[21] Hu B and Tekić J 2007 *Phys. Rev.* E **75** 056608
[22] Tekić J and Hu B 2008 *Phys. Rev.* B **78** 104305
[23] Hirano M, Shinjo K, Kaneko R and Murata Y 1997 *Phys. Rev. Lett.* **78** 1448
[24] Dienwiehel M, Verhoeven G S, Pradeep N, Frenken J W M, Heimberg J A and Zandbergen H W 2004 *Phys. Rev. Lett.* **92** 126101
[25] Persson B N J 1998 *Sliding Friction: Physical Principles and Applications* (Berlin: Springer-Verlag)
[26] Persson B N J 1999 *Surf. Sci. Rep.* **33** 83